Electrocaloric properties of ferroelectric-paraelectric superlattices controlled by the thickness of paraelectric layer in a wide temperature range

D. C. Ma, S. P. Lin, W. J. Chen, Yue Zheng', Biao Wang', and W. M. Xiong

Citation: AIP Advances **4**, 107144 (2014); doi: 10.1063/1.4900858
View online: http://dx.doi.org/10.1063/1.4900858
View Table of Contents: http://aip.scitation.org/toc/adv/4/10
Published by the American Institute of Physics

Electrocaloric properties of ferroelectric-paraelectric superlattices controlled by the thickness of paraelectric layer in a wide temperature range

D. C. Ma,[1,3] S. P. Lin,[1,3] W. J. Chen,[2,3] Yue Zheng,[2,3,a] Biao Wang,[2,b] and W. M. Xiong[2,3]

[1]*Sino-French Institute of Nuclear Engineering and Technology, Sun Yat-Sen University, Guangzhou 510275, China*

[2]*State Key Laboratory of Optoelectronic Materials and Technologies, Sun Yat-sen University, Guangzhou 510275, China*

[3]*Micro&Nano Physics and Mechanics Research Laboratory, School of Physics and Engineering, Sun Yat-sen University, Guangzhou 510275, China*

(Received 6 August 2014; accepted 20 October 2014; published online 28 October 2014)

As functions of the paraelectric layer thickness, misfit strain and temperature, the electrocaloric properties of ferroelectric-paraelectric superlattices are investigated using a time-dependent Ginzburg-Landau thermodynamic model. Ferroelectric phase transition driven by the relative thickness of the superlattice is found to dramatically impact the electrocaloric response. Near the phase transition temperature, the magnitude of the electrocaloric effect is maximized and shifted to lower temperatures by increasing the relative thickness of paraelectric layer. Theoretical calculations also imply that the electrocaloric effect of the superlattices depends not only on the relative thickness of paraelectric layer but also on misfit strain. Furthermore, control of the relative thickness of paraelectric layer and the misfit strain can change availably both the magnitude and the temperature sensitivity of the electrocaloric effect, which suggests that ferroelectric-paraelectric superlattices may be promising candidates for use in cooling devices in a wide temperature range. [http://dx.doi.org/10.1063/1.4900858]

I. INTRODUCTION

Electrocaloric (EC) effect has generated increasing interest for application in solid-state cooling devices over the past decades.[1–13] EC effect is intimately connected to the change of entropy by applying external electric field.[1–8] Even though the external electric field can result in a non-dissipative temperature change of a material, caloric effects are expected to be maximized in the vicinity of a transition point. Recently, a giant EC effect was found in the ferroelectric thin films (FTFs) near the temperatures of phase transitions at which the spontaneous polarization undergoes a dramatic change with temperature.[3] The coupling between electric and thermal fields in ferroelectric materials gives rise to the giant EC effect. For practical cooling devices, it is important to find a kind of ferroelectric material which is easy to control the transition temperature, high thermal efficiency, efficient heat transfer, large breakdown fields and so on.

EC cooling, based on electric-field-driven temperature changes near phase transitions of ferroelectric materials, is a candidate solid-state cooling technology. For bulk material,[9] EC effects are small because they can only bear low breakdown fields and heat transfer is inefficient owing to low surface-to-volume ratio. FTFs, possessing large breakdown fields, are confirmed to show large EC effect by experiments and theory.[3,5] However, FTFs cannot pump significant heat and the heat is often thermally absorbed by substrates. Ferroelectric multilayer structures (FMSs), consisting of many

[a]Author to whom correspondence should be addressed. Electronic address: zhengy35@mail.sysu.edu.cn
[b]Electronic address: wangbiao@mail.sysu.edu.cn

FTFs, have been proposed as the promising candidates forward towards practical EC cooler.[10–12] Giant EC effect can be achieved in FMSs with efficient heat transfer due to the large surface-to-volume ratio of the constituent FTFs.[13] FMSs have been shown to overcome the disadvantages identified in bulk and films while preserving all of the corresponding advantages. Therefore FMS represents the optimal geometry for EC cooling applications.

Artificially structured ferroelectric superlattices are a class of new functional ferroelectric material systems which give new opportunities for novel applications. Over the past decades, some studies of systems such as $KNbO_3/KTaO_3$,[14] $PbTiO_3/SrTiO_3$,[15] $BaTiO_3/SrTiO_3$[16] and $PbTiO_3/BaTiO_3$, etc., have revealed that their phase transition temperatures, domain pattern, polarization and susceptibilities were determined by interfacial and other related properties such as structural periodicity, misfit strain, electrostatic interactions and electro-mechanical boundary conditions. Therefore, transition temperatures of ferroelectric-paraelectric superlattices (FPS), such as $BaTiO_3/SrTiO_3$ (BT/ST) and $PbTiO_3/SrTiO_3$ (PT/ST), etc., grown epitaxially on ST substrate were shown to depend on the relative thickness of ferroelectric or paraelectric layers. If the thickness or ratio of the PT layers is below certain critical values, the ferroelectricity of superlattices would disappear as shown by Dawber[15] *et al*. and Chen[16] *et al*. Our previous phase-field study also revealed that the thicker ST layers were, the lower transition temperatures were.[17]

Theoretically, the thermodynamic model based on Landau theory has been developed to predict the EC effect of FTFs, nanoparticle and multilayer. In this paper, we employ time-dependent Ginzburg-Landau (TDGL) theory to investigate the EC effect of FPS. The adiabatic temperatures are calculated as functions of the relative thickness of paraelectric layer, applied electric field, misfit strain and temperature. The simulations show that the magnitude of the EC effect in FPS and its dependence on temperature can be controlled by the relative thickness of paraelectric layer and misfit strain. In other words, we could obtain the desired EC effect of FPS through carefully choosing the thickness of PT and ST layer and substrate materials.

II. SIMULATION METHODOLOGY

We consider as our thermodynamic reference a crystal of infinite extent absent an applied field, i.e., electric, magnetic, or mechanical (internal or external). The total polarization $\mathbf{P}^{\mathrm{T}}$ for ferroelectric can be separated into the spontaneous polarization $\mathbf{P}$ and the polarization induced by the electric field $\mathbf{P}^{\mathrm{E}}$, i.e. $\mathbf{P}^{\mathrm{T}}=\mathbf{P}+\mathbf{P}^{\mathrm{E}}$.[18–22] To the lowest order, $\mathbf{P}^{\mathrm{E}}$ is linearly proportional to the electric field $\mathbf{E}$ and can be written as $\mathbf{P}^{\mathrm{E}}=\boldsymbol{\chi}_{\mathrm{b}}\mathbf{E}$, here $\boldsymbol{\chi}_{\mathrm{b}}$ are the background susceptibility tensor of the reference crystal far from any lattice instability.[18–22] Therefore, the electric displacement field $\mathbf{D}$ at constant applied stress and temperature can be expressed in terms of the linear-part induced polarization $\mathbf{P}^{\mathrm{E}}$ and the non-linear-part spontaneous polarization $\mathbf{P}$ as $\mathbf{D} = \varepsilon_0\mathbf{E} + \mathbf{P}^{\mathrm{T}} = \varepsilon_0\mathbf{E} + \mathbf{P}^{\mathrm{E}} + \mathbf{P} = \varepsilon_0\mathbf{E} + \boldsymbol{\chi}_{\mathrm{b}}\mathbf{E} + \mathbf{P} = \boldsymbol{\varepsilon}_{\mathrm{b}}\mathbf{E} + \mathbf{P}$, where ε_0 is the vacuum permittivity and $\boldsymbol{\varepsilon}_{\mathrm{b}} \equiv \varepsilon_0 + \boldsymbol{\chi}_{\mathrm{b}}$ is the background dielectric constant tensor. Since the background material is the paraelectric phase of a cubic crystal structure, the background dielectric constants in three axis directions are the same, i.e., $\varepsilon_{\mathrm{b}} = \varepsilon_{11\mathrm{b}} = \varepsilon_{22\mathrm{b}} = \varepsilon_{33\mathrm{b}}$.

We consider a FPS made of multilayer thin films sandwiched between electrodes and grown epitaxially on a compressive substrate, as shown in Fig. 1. A coordinate system is used in which the x_1 axis is parallel to [1 0 0], the x_2 axis to [0 1 0], and the x_3 axis to [0 0 1]. The superlattice in the x_1 and x_2 directions extends to infinity, and the interface between slab A and B is located at x_3=0 (Fig. 1(b)). The multilayer thin films is composed of alternating layers of slab A and B of thickness h_{A} and h_{B}, respectively, with total thickness much larger than the thickness H of a single period of the superlattice, i.e. $H=h_{\mathrm{A}} + h_{\mathrm{B}}$. Our theoretical description is based on the phase-field method coupled with microelasticity and electrostatics. In this approach, we take the spontaneous polarization vector, $\mathbf{P}^m = \left(P_1^m, P_2^m, P_3^m\right)$, as the order parameter, where m=A, B. Following the previous works,[10,16,17,22] the spontaneous polarization $\mathbf{P}^m(x_i)$ for a given temperature and time can be solved from the TDGL equations,

$$\frac{\partial \mathbf{P}^m(x_i,t)}{\partial t} = -L\frac{\delta F}{\delta \mathbf{P}^m(x_i,t)}, \tag{1}$$

where L is the kinetic coefficient, t is time and F is the total free energy of a single period of the

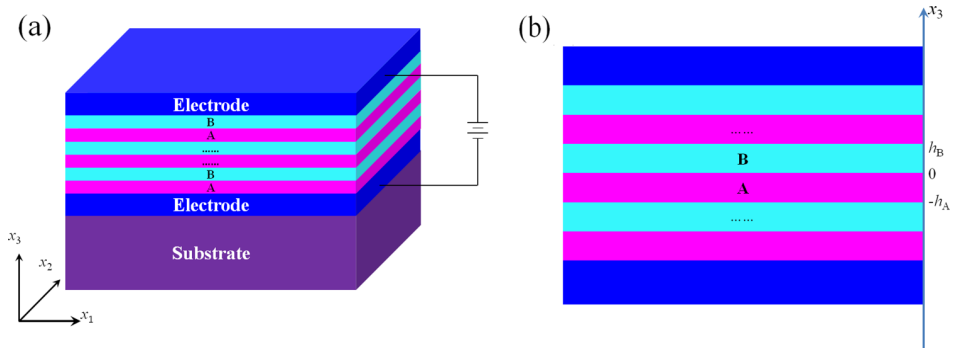

FIG. 1. Schematic structures of (a) an epitaxial A/B superlattice on a substrate and (b) the simulation cell.

simulated FPS system, i.e., $F = F^{A} + F^{B}$ where F^{A} and F^{B} are the free energy of A and B layer, respectively. The free energy of a single layer F^{m} includes bulk free energy F^{m}_{Bulk}, elastic energy F^{m}_{Ela}, domain wall energy F^{m}_{G}, electric energy F^{m}_{E} and interfacial energy F^{m}_{I}, which has the expression[18,23]

$$\begin{aligned} F^{m} &= F^{m}_{\text{Bulk}} + F^{m}_{\text{Ela}} + F^{m}_{\text{G}} + F^{m}_{\text{E}} + F^{m}_{\text{I}} \\ &= \iiint_{V} \left(f^{m}_{\text{Bulk}} + f^{m}_{\text{Ela}} + f^{m}_{\text{G}} + f^{m}_{\text{E}}\right) dV + \iint_{S} f^{m}_{\text{I}} dS \end{aligned} \tag{2}$$

where f^{m}_{Bulk}, f^{m}_{Ela}, f^{m}_{G} and f^{m}_{E} are the bulk free energy density, elastic energy density, domain wall energy density, and electric energy densities, respectively, in the m-layer. f_{I} is the interfacial energy density. V is the volume of the superlattice. For a superlattice epitaxially grown on substrate, the sum of its bulk free energy density f^{m}_{Bulk} and elastic energy density f^{m}_{Ela} is given by[24–29]

$$\begin{aligned} f^{m}_{\text{Bulk}} + f^{m}_{\text{Ela}} &= \alpha^{m*}_{1}\left[\left(P^{m}_{1}\right)^{2} + \left(P^{m}_{2}\right)^{2}\right] + \alpha^{m*}_{3}\left(P^{m}_{3}\right)^{2} + \alpha^{m*}_{11}\left[\left(P^{m}_{1}\right)^{4} + \left(P^{m}_{2}\right)^{4}\right] \\ &+ \alpha^{m*}_{33}\left(P^{m}_{3}\right)^{4} + \alpha^{m*}_{12}\left(P^{m}_{1}\right)^{2}\left(P^{m}_{2}\right)^{2} + \alpha^{*}_{13m}\left[\left(P^{m}_{1}\right)^{2} + \left(P^{m}_{2}\right)^{2}\right]\left(P^{m}_{3}\right)^{2} \\ &+ \alpha^{m}_{111}\left[\left(P^{m}_{1}\right)^{6} + \left(P^{m}_{2}\right)^{6} + \left(P^{m}_{3}\right)^{6}\right] + \alpha^{m}_{112}\Big\{\left(P^{m}_{1}\right)^{4}\left[\left(P^{m}_{2}\right)^{2} + \left(P^{m}_{3}\right)^{2}\right], \\ &+ \left(P^{m}_{2}\right)^{4}\left[\left(P^{m}_{1}\right)^{2} + \left(P^{m}_{3}\right)^{2}\right] + \left(P^{m}_{3}\right)^{4}\left[\left(P^{m}_{1}\right)^{2} + \left(P^{m}_{2}\right)^{2}\right]\Big\} \\ &+ \alpha^{m}_{123}\left(P^{m}_{1}\right)^{2}\left(P^{m}_{2}\right)^{2}\left(P^{m}_{3}\right)^{2} + \frac{\left(u^{m}_{\text{mis}}\right)^{2}}{s^{m}_{11} + s^{m}_{12}} \end{aligned} \tag{3}$$

where the renormalized coefficients is expressed as

$$\begin{aligned} \alpha^{m*}_{1} &= \alpha^{m}_{1} - u^{m}_{\text{mis}}\frac{Q^{m}_{11} + Q^{m}_{12}}{s^{m}_{11} + s^{m}_{12}},\ \alpha^{m*}_{3} = \alpha^{m}_{1} - u^{m}_{\text{mis}}\frac{2Q^{m}_{12}}{s^{m}_{11} + s^{m}_{12}}, \\ \alpha^{m*}_{11} &= \alpha^{m}_{11} + \frac{\left\{\left[\left(Q^{m}_{11}\right)^{2} + \left(Q^{m}_{12}\right)^{2}\right]s^{m}_{11} - 2Q^{m}_{11}Q^{m}_{12}s^{m}_{12}\right\}}{2\left[\left(s^{m}_{11}\right)^{2} - \left(s^{m}_{12}\right)^{2}\right]}, \\ \alpha^{m*}_{12} &= \alpha^{m}_{12} - \frac{\left\{\left[\left(Q^{m}_{11}\right)^{2} + \left(Q^{m}_{12}\right)^{2}\right]s^{m}_{12} - 2Q^{m}_{11}Q^{m}_{12}s^{m}_{11}\right\}}{\left[\left(s^{m}_{11}\right)^{2} - \left(s^{m}_{12}\right)^{2}\right]} + \frac{\left(Q^{m}_{44}\right)^{2}}{2s^{m}_{44}}, \\ \alpha^{m*}_{13} &= \alpha^{m}_{12} + \frac{Q^{m}_{12}\left(Q^{m}_{11} + Q^{m}_{12}\right)}{s^{m}_{11} + s^{m}_{12}},\ \alpha^{m*}_{33} = \alpha^{m}_{11} + \frac{\left(Q^{m}_{12}\right)^{2}}{s^{m}_{11} + s^{m}_{12}}, \end{aligned} \tag{4}$$

where α^{m}_{i}, α^{m}_{ij} and α^{m}_{ijk} are dielectric stiffness coefficients at constant stress, the Q^{m}_{ij} is electrostrictive coefficients and s^{m}_{ij} is elastic compliances at constant polarization for the m-layer. u^{m}_{mis} is misfit strain generated by the lattice mismatch between the layer and the underlying substrate, i.e. $u^{m}_{\text{mis}} = (a_{\text{s}}\text{-}a_{m})/a_{\text{s}}$, where a_{s} is the substrate lattice parameter and a_{m} is cubic cell constant of the free standing m-layer film.

The domain wall energy, which presents the contribution of the domain walls to the total free energy, is introduced through the gradient of the polarization field.[30] This gradient energy density f_{G}^{m} in superlattice can be written as[16,17,31]

$$\begin{aligned} f_{\mathrm{G}}^{m} &= \frac{1}{2}G_{11}^{m}\left[\left(P_{1,1}^{m}\right)^{2}+\left(P_{2,2}^{m}\right)^{2}+\left(P_{3,3}^{m}\right)^{2}\right]+G_{12}^{m}\left(P_{1,1}^{m}P_{2,2}^{m}+P_{2,2}^{m}P_{3,3}^{m}+P_{1,1}^{m}P_{3,3}^{m}\right) \\ &+ \frac{1}{2}G_{44}^{m}\left[\left(P_{1,2}^{m}+P_{2,1}^{m}\right)^{2}+\left(P_{2,3}^{m}+P_{3,2}^{m}\right)^{2}+\left(P_{1,3}^{m}+P_{3,1}^{m}\right)^{2}\right] \\ &+ \frac{1}{2}G_{44}^{m'}\left[\left(P_{1,2}^{m}-P_{2,1}^{m}\right)^{2}+\left(P_{2,3}^{m}-P_{3,2}^{m}\right)^{2}+\left(P_{1,3}^{m}-P_{3,1}^{m}\right)^{2}\right] \end{aligned} \tag{5}$$

where G_{ij}^{m} and $G_{ij}^{m'}$ are the gradient energy coefficients of the m-layer, and the commas in the subscripts denote spatial differentiation.

According to the previous works[18–20,31,32] the electric energy density of a given polarization distribution is expressed as

$$f_{\mathrm{E}}^{m} = -E_{i}^{m}P_{i}^{m}-\frac{1}{2}\varepsilon_{\mathrm{b}}E_{i}^{m}E_{i}^{m} \tag{6}$$

Taking interfacial coupling between layers A and B into account, the boundary conditions for the polarizations at the interfaces x=0 are

$$\begin{aligned} \left.\frac{dP_{i}^{A}}{dx_{3}}\right|_{x_{3}=0^{-}} &= -\frac{P_{i}^{A}(0)}{\delta_{i}^{A}}+\frac{\xi_{i}P_{i}^{B}(0)}{D_{ij}^{A}} \\ \left.\frac{dP_{i}^{B}}{dx_{3}}\right|_{x_{3}=0^{+}} &= \frac{P_{i}^{B}(0)}{\delta_{i}^{B}}-\frac{\xi_{i}P_{i}^{A}(0)}{D_{ij}^{B}} \end{aligned} \tag{7}$$

where δ_{i}^{m} is the so-called extrapolation length of m-layer, which describes the difference between the surface and the interior, ξ_{i} describes the short-range coupling strength between layer A and layer B, D_{ij}^{m} is the material coefficients related to the gradient energy coefficients of m-layer. The periodic boundary conditions for the polarizations of an infinite superlattice structure can be described by

$$\begin{aligned} \left.\frac{dP_{i}^{A}}{dx_{3}}\right|_{x_{3}=-h_{A}} &= \frac{P_{i}^{A}(-h_{A})}{\delta_{i}^{A}}-\frac{\xi_{i}P_{i}^{B}(h_{B})}{D_{ij}^{A}} \\ \left.\frac{dP_{i}^{B}}{dx_{3}}\right|_{x_{3}=h_{B}} &= -\frac{P_{i}^{B}(h_{B})}{\delta_{i}^{B}}+\frac{\xi_{i}P_{i}^{A}(-h_{A})}{D_{ij}^{B}} \end{aligned} \tag{8}$$

After further derivations obtained from Maxwell relations, as a uniform electric field is applied to a dielectric solid, the EC coefficient is described as[4,5,33]

$$p_{i} = \left(\frac{\partial S}{\partial E_{i}}\right)_{T} = \left(\frac{\partial D_{i}}{\partial T}\right)_{E} \tag{9}$$

The adiabatic temperature change ΔT in the dielectric material due to a change in external electric field is written by

$$\Delta T = -\frac{T}{C_{E}}\int_{E_{a}}^{E_{b}}\left(\frac{\partial D_{i}}{\partial T}\right)_{E}dE \tag{10}$$

where C_{E} is the heat capacity per unit volume at constant electric field, E_{a} and E_{b} are the starting and final applied fields, respectively.

If a ferroelectric solid solution is considered in infinite dimensions, the electric field E is equivalent to the external electric field. One can calculate the EC effect of the ferroelectric solid solution using Eq. (9) and Eq. (10). However, for ferroelectric nanostructures, the total electric field E_{i} originates from the external electric field E_{i}' and the depolarization field E_{i}^{d} determined by the inhomogeneous distribution of the spontaneous polarization in ferroelectrics or incomplete charge compensation of electrodes, i.e. $E_{i} = E_{i}' + E_{i}^{\mathrm{d}}$.[34–37] Then the electric displacement may be rewritten

in the form,

$$D_i = \varepsilon_b E_i + P_i = \varepsilon_b E_i' + \varepsilon_b E_i^d + P_i \tag{11}$$

By considering that E_i' is independent on temperature and E_i^{d} is a function of temperature, we redefine the EC coefficient of the ferroelectric nanostructures caused by the external electric field as,

$$p_i = \left[\frac{\partial(\varepsilon_b E_i^d + P_i)}{\partial T}\right]_{E'} = \left(\frac{\partial P_i^0}{\partial T}\right)_{E'} \tag{12}$$

where $P_i^0 = \varepsilon_b E_i^d + P_i$ is the electric displacement component dependent on temperature and is actually measured in experiment of EC effect. Thus, adiabatic temperature change is rewritten as,

$$\Delta T = -\frac{T}{C_E}\int_{E_a}^{E_b}\left(\frac{\partial P_i^0}{\partial T}\right)_{E'} dE' \tag{13}$$

In general case, especially with bulk materials or thicker films, the p_i is known as $(\partial <P_i> / \partial T)_{\sigma,E}$, where the total electric field E only includes the external filed, because the depolarization field is very small, and $\varepsilon_b E_i^d$ is much more less than P_i. But it is not suited for all cases. For ultra-thin FTFs, superlattices and multilayers etc., the depolarization filed becomes very large, and can't be neglected. Effect of the depolarization filed on EC effect of ferroelectrics should be considered. For representing accurately our simulation, we take Eq. (12) and Eq. (13) to evaluate the EC effect of PT/ST superlattices.

In our simulation, we investigate FPS that consist of $PbTiO_3$ (PT) and $SrTiO_3$ (ST). We consider PT and ST as slab A and slab B, respectively. In order to calculate the equilibrium polarization of PT/ST superlattices, all of the intrinsic material property coefficients entering into the above relations for PT and ST were taken from reference.[16,17,24,38] The calculations consider only cases in which the PT/ST superlattice is fully commensurate with the substrate, and the misfit strains arising from the substrate constraint are uniform and in-planar. Therefore, the misfit strains of PT and ST layers can be given by $u_{\mathbf{mis}}^{\mathrm{A}} = (a_{\mathrm{S}}\text{-}a_{\mathrm{A}})/a_{\mathrm{S}}$ and $u_{\mathbf{mis}}^{\mathrm{B}} = (a_{\mathrm{S}}\text{-}a_{\mathrm{B}})/a_{\mathrm{S}}$. The absolute value of the heat capacity of PT and ST layers is approximately constant as 3.05×10^6 J/m^{3}K and 2.78×10^6 J/m^{3}K in our simulation, respectively. We solve the above equations numerically using the finite difference method. The superlattice is represented by $N_1\Delta x_1 \times N_2\Delta x_2 \times N_3\Delta x_3$ along the x_1, x_2, x_3 directions, in which Δx_1, Δx_2 and Δx_3 are the finite length, N_1, N_2 and N_3 are the total number of x_1, x_2 and x_3 grid, respectively. To simulate the electrocaloric effect of PT/ST superlattice, the mean polarization of the simulation system was calculated from the formula $<P_i^0>= \frac{(1-\alpha)}{V_A}\iiint_{V_A} P_i^{A0} dV_A + \frac{\alpha}{V_B}\iiint_{V_B} P_i^{B0} dV_B$, where α is the relative thickness of ST layers, i.e. $\alpha = h_{\mathrm{B}}/(h_{\mathrm{A}} + h_{\mathrm{B}})$, V_{A} and V_{B} are the volume of A and B layer, respectively.

III. RESULTS AND DISCUSSION

A. The electrocaloric effect of FPS

To investigate the electrocaloric effect of PT/ST superlattice with a change external electric field, we employ a simulation cell of $64\Delta x_1 \times 64\Delta x_2 \times N_3\Delta x_3$ where $\Delta x_1 = \Delta x_2 = \Delta x_3 = 1$ nm. Fig. 2 shows the temperature dependence of $<P_3^0>$ and its derivative with respect to temperature under different external electric fields with the compressive strain of $u_{\mathrm{mis}}^{\mathrm{A}} = -0.016$ and $u_{\mathrm{mis}}^{\mathrm{B}} = 0$ as the relative thickness of ST layer α is 0.5. Under the large compressive strain, the in-plane polarization are suppressed and only the out-plane polarization along the x_3 axis exists, which is consistent with the previous results of superlattices.[17,27] As a result of the strong electrostatic coupling between the PT and ST layers, the $<P_3^0>$ in case of α=0.5 is smaller than that in case of α=1 under the zero field in PT/ST superlattices (see Fig. 2(a)). In addition, from Fig. 2(b), the zero field ferroelectric to paraelectric transition is 592K at α=0.5, which is lower comparing with 1106K at α=1. Moreover, the applied electric field undoubtedly results in an enhancement of average polarization and induces the transition from paraelectric phase to a ferroelectric phase. Due to the compressive strain, in

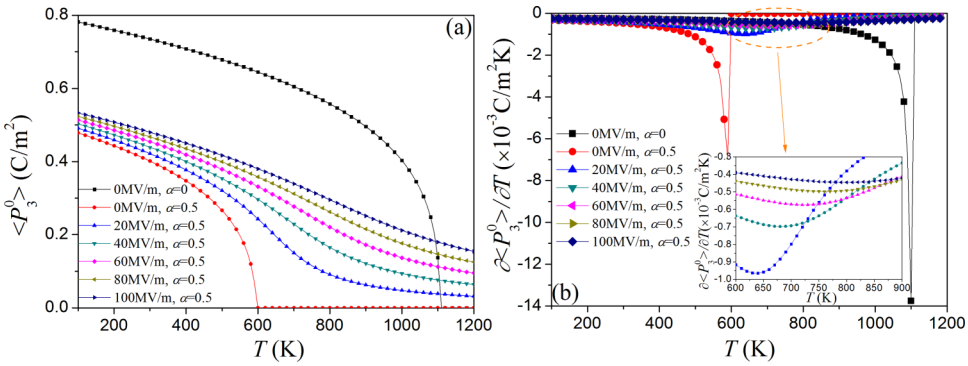

FIG. 2. Temperature dependence of (a) the $<P_3^0>$ and (b) its derivative with respect to temperature of the PT/ST superlattices in which the relative thickness of ST layer is 0.5 with different applied electric fields.

the epitaxial thin film and superlattice, the polarization is enhanced and the transition temperature rises.[31,39,40] When the working temperature is larger than 100K, bulk PT and ST are, respectively, ferroelectric and paraelectric.[41] However, because the polarization of the ST layers can be induced by the spontaneous polarization in the PT layer by mean of depolarization field in superlattices, the average polarization or transition temperature is smaller than that of the PT thin film.[16–18,27]

Using Eq. (13), the adiabatic temperature change (ΔT) in superlattices due to the applied field change can be determined as a function of temperature for different external electrical field changes $\Delta E'$, as shown in Fig. 3. From Fig. 2, Fig. 3(a) and 3(b), the ΔT_{Max} shows up near the phase transition temperature, which is in agreement with the previous works.[1,3,5] As expected from Eq. (13), in the

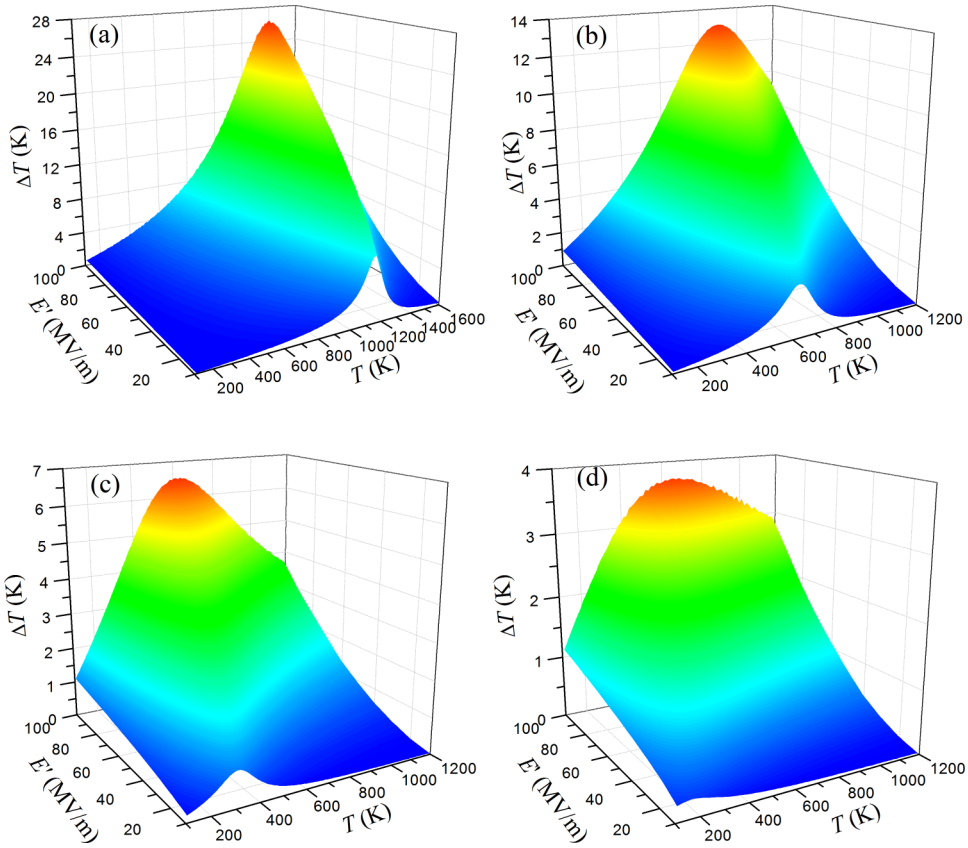

FIG. 3. Adiabatic temperature change ΔT as a function of temperature under various applied electric fields at (a) α=0, (b) α=0.5, (c) α=0.8 and (d) α=1 in PT/ST superlattice.

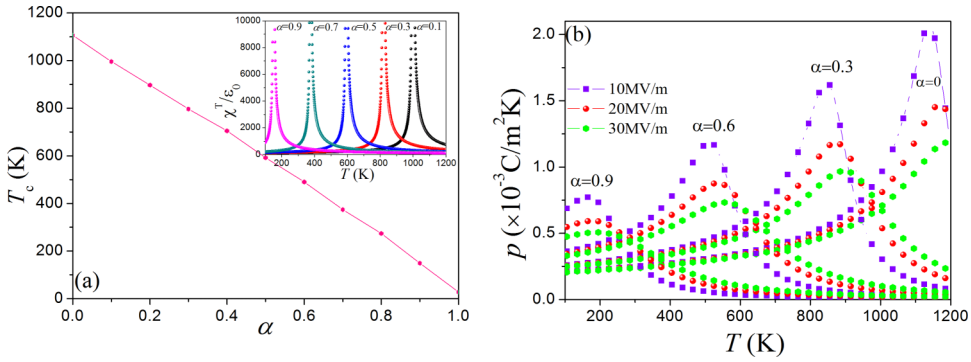

FIG. 4. The dependence of (a) transition temperature T_c and (b) EC coefficient p at $\Delta E'$=10, 20 and 30MV/m with the various relative thickness of ST layer in PT/ST superlattice.

PT/ST superlattices, an increase in the $\Delta E'$ at constant temperature leads to a linear increase in the magnitude of the temperature change ΔT due to the electrocaloric effect. It is noted that the temperature T_{Max} where this change in thermal temperature is largest increases significantly with the enhancement of external electric field, which is consistent with the FTF.[5,42] In addition, from Fig. 3, it is found that the increase of α has an ability to drop down the temperature T_{Max} and the T_{Max} reach to room temperature at $\Delta E'$ = 10 MV/m and α=0.8 (Fig. 3(c)). Likewise, the adiabatic temperature changes (ΔT) are falling partly while the relative thickness of ST layers α increases.

B. Influence of the ST layer relative thickness on EC effect

From the above results, the ΔT_{Max} of PT/ST superlattices appears at the phase transition temperature when the external electric field is applied. So the working temperature of the EC effect in the superlattices can be tuned by controlling the transition temperature. According to the previous work,[17] the transition temperature of the PT/ST superlattices can be determined and controlled by the relative thickness of the ST layer α. Based on the results, the dependence of transition temperature on the value of α is shown in Fig. 4(a) at zero applied electric field. In the curve of Fig. 4(a), the transition temperature decreases monotonously with the value of α increasing. The results indicate that we can choose easily the working temperature of FPS for use in practice. Fig. 4(b) show the p-T curve for different the value of α due to applied $\Delta E'$. In Fig. 4(b), it can be seen that the maximum EC coefficient p_{max} move toward lower temperature with the value of α increasing. In addition, the comparison of EC effect between the ferroelectric and paraelectric phases, the EC coefficient in ferroelectric phase is much larger than that in the paraelectric phase. It is shown that the transition

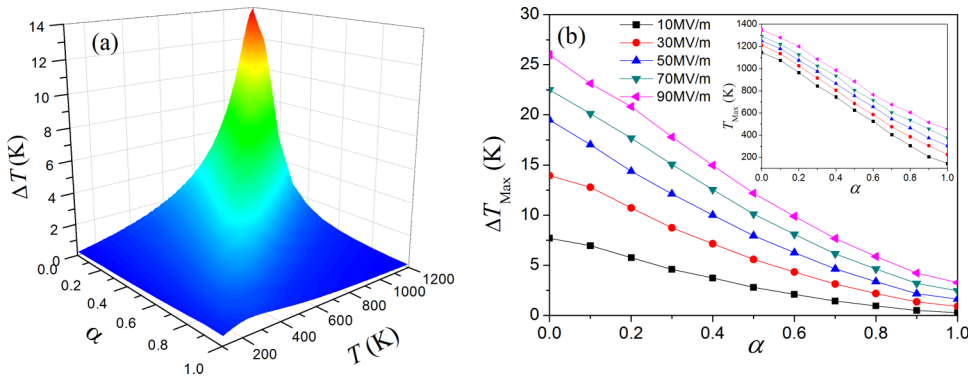

FIG. 5. (a) Three-dimensional distribution of the EC effect for various relative thicknesses of ST layer and temperatures in PT/ST superlattices with the applied $\Delta E'$=10MV/m. (b) The maximum change of thermal temperature ΔT_{Max} and the temperature T_{Max} as functions of the relative thickness of ST layer at different electric field changes $\Delta E'$.

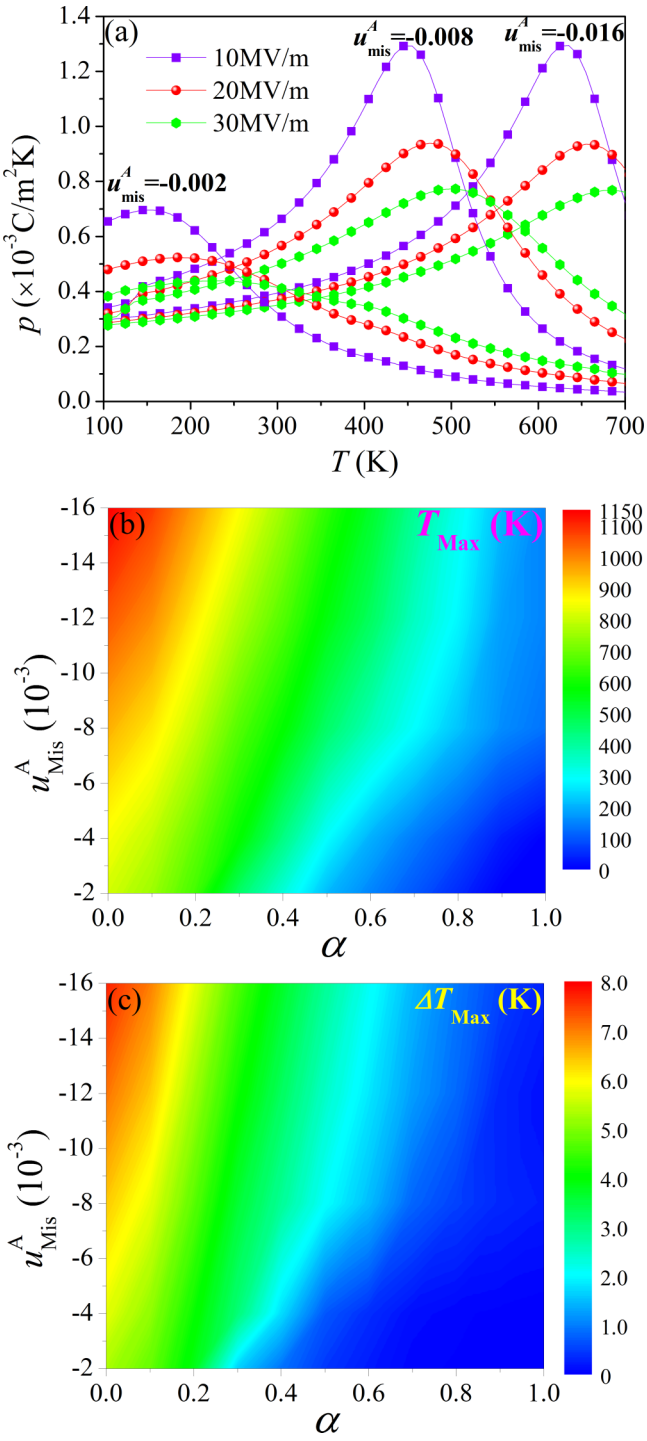

FIG. 6. (a) The EC coefficient p due to applied $\Delta E'$ as a function of temperature T in PT/ST superlattices with different misfit strain of PT layer: -0.002, -0.008 and -0.016. Pseudocolor plots of (b) the T_{Max} and (c) ΔT_{Max} of PT/ST superlattices as functions of the relative thickness of ST layer and misfit strain of PT layer at $\Delta E'$=10MV/m.

temperature in the PT/ST superlattices can be tuned by the relative thickness of the ST layer, which suggests artificial tuning of working temperature of the superlattices is possible.

It will also be considered that the EC effect is tuned by varying the value of α in superlattices. Three-dimensional distribution of the EC effect for the different α and temperature is shown in Fig. 5(a) at $\Delta E'$=30 MV/m. From Fig. 5(a), the maximum value of EC effect is not only dependent

on temperature and external electric field, but also strongly related to the relative thickness of ST layer. As a consequence of the influence of the relative thickness of ST layer on the EC effect, an increase of the ST layer relative thickness shifts the maximum in the EC effect to lower temperatures and reduces its magnitude.[15–17] Conversely, a decrease of the ST layer relative thickness shifts the maximum in the EC effect to higher temperatures and increases its magnitude. It is shown more clearly in Fig. 5(b) that the ΔT_{Max} and T_{Max} are plotted with the relative thickness of ST layer. In Fig. 5(b), we see that the ΔT_{Max} and T_{Max} depend linearly on the relative thickness of ST layer. Since the polarization of the system comes from the spontaneous polarization of the PT layer, increasing the ratio of ST and PT layer thicknesses from 0 to 1 enhances the depolarization and results in the reduction of the spontaneous polarization in the PT layer and transition temperature of the system. Note that the electric-field-induced T_{Max} shift is still observed in FPS with the change of α.

C. Mechanical regulation of EC effect in FPS

To investigate the mechanical regulation on EC effect of PT/ST superlattices, the misfit strain of PT layer is changed. Fig. 6(a) shows the EC coefficient p as a function of temperature T in PT/ST superlattices with different misfit strain of PT layer at $\Delta E'$=10MV/m, 20MV/m and 30MV/m while the relative thickness of ST layer is 0.5. The results in Fig. 6(a) indicate that both the magnitude of the EC effect of FPS as measured by p and the temperature T_{max} at which it is maximized do depend on the misfit strain. The temperature T_{Max} is decreases significantly while the PT layers are subjected to a compressive misfit strain from u_m^A=-0.016 to -0.002 and the misfit strain of ST layers is simultaneously changed from u_m^B=0 to 0.014. When the misfit strain of PT layers is more compressive, the transition temperature is raised due to the enhanced out-plane polarization through electrostriction while under reduced compressive misfit strain of PT layers the out-plane polarization is suppressed causing the phase transition to occur at lower temperatures by increasing tensile misfit strain of ST layers.

From above the results, the EC effect of a FPS is a function of both the misfit strain and the relative thickness of ST layer α. It is clearly shown in Fig. 6(b) and Fig. 6(c) where the change of the T_{Max} and ΔT_{Max} in FPS are drawn at different misfit strains u_m^A together with the relative thickness of ST layer for the change in applied electric field 10MV/m. As expected, the T_{Max} and ΔT_{Max} exhibit a nearly linear decrease as the misfit strain of PT layers and relative thickness of ST layer are varied from -0.016 to -0.002 and from 0 to 1, respectively. Consequently by appropriately choosing both the relative thickness of the ST layer and substrate materials, the magnitude and temperature dependence of the EC effect can be controlled within a wide range.

IV. CONCLUSION

In summary, a thermodynamic model based on the time-dependence Ginzburg-Landau (TDGL) theory is employed to investigate the electrocaloric (EC) effect of ferroelectric-paraelectric superlattices (FPS). The magnitude of EC effect induced by external electric field exhibits a peak only at the temperature close to transition temperature, which is similar to that of the ferroelectric thin film (FTF). Our results also indicate the magnitude of EC effect shifts to lower temperatures with increasing the relative thickness of paraelectric layer. The theoretical simulation also shows that the EC effect, including the temperature sensitivity and magnitudes, strongly depends not only on the relative thickness of the ST layer but also on the misfit strain. This work suggests that we could obtain the desired EC effect through carefully choosing the relative thickness of the ST layer and substrate material. It may bring more opportunities for practical application in cooling systems.

ACKNOWLEDGMENTS

We acknowledge the financial support of the National Natural Science Foundation of China (NSFC) (Nos. 11372361, 11302268, 51172291, 11474363, 11232015). Yue Zheng also thanks support by the Fundamental Research Funds for the Central Universities, NCET in University,

Research Fund for the Doctoral Program of Higher Education, Fok Ying Tung Foundation, Science and Technology Innovation Project of Guangdong Provincial Education Department and Guangdong Natural Science Funds for Distinguished Young Scholar, the Fundamental Research Funds for the Central Universities.

[1] M. C. Rose and R. E. Cohen, Phys. Rev. Lett. **109**, 187604 (2012).
[2] S. Kar-Narayan, S. Crossley, X. Moya, V. Kovacova, J. Abergel, A. Bontempi, N. Baier, E. Defay, and N. D. Mathur, Appl. Phys. Lett. **102**, 032903 (2013).
[3] A. S. Mischenko1, Q. Zhang, J. F. Scott, R. W. Whatmore, and N. D. Mathur, Science **311**, 70 (2006).
[4] T. Correia and Q. Zhang, "Electrocaloric materials: new generation of coolers," *Engineer materials* (Springer, Berlin, 2014), Vol. 34.
[5] Y. Liu, X. P. Peng, X. J. Lou, and H. Zhou, Appl. Phys. Lett. **100**, 192902 (2002).
[6] J. Wang, M. Liu, Y. J. Zhang, T. Shimada, S. Q. Shi, and T. Kitamura, J. Appl. Phys. **115**, 164102 (2014).
[7] J. F. Scott, Science **315**, 954 (2007).
[8] X. Moya, S. Kar-Narayan1, and N. D. Mathur, Nat. Mater. **103**, 024104 (2008).
[9] R. B. Olsen, W. F. Butler, D. A. Payne, B. A. Tuttle, and P. C. Held, Phys. Rev. Lett. **45**, 1436 (1980).
[10] B. Li, J. B. Wang, X. L. Zhong, F. Wang, B. L. Liu, X. J. Lou, and Y. C. Zhou, Europhys. Lett. **95**, 67004 (2011).
[11] J. H. Qiu, J. N. Ding, N. Y. Yuan, X. Q. Wang, and J. Yang, Solid State Commun. **152**, 856 (2012).
[12] J. H. Qiu and Q. Jiang, Solid State Commun. **149**, 1549 (2009).
[13] S. Kar-Narayan and N. D. Mathur, Appl. Phys. Lett. **95**, 242903 (2009).
[14] J. Sigman, D. P. Norton, and H. M. Christen, Phys. Rev. Lett. **88**, 097601 (2002).
[15] M. Dawber, C. Lichtensteiger, M. Cantoni, M. Veithen, P. Ghosez, K. Johnston, K. M. Rabe, and J. M. Triscone, Phys. Rev. Lett. **95**, 177601 (2005).
[16] Y. L. Li, S. Y. Hu, D. Tenne, A. Soukiassian, D. G. Schlom, and X. X. Xi, Appl. Phys. Lett. **91**, 112914 (2007).
[17] D. C. Ma, Y. Zheng, and C. H. Woo, Acta Mater. **57**, 4736 (2009).
[18] Y. Zheng and C. H. Woo, Appl. Phys. A **97**, 617 (2009).
[19] J. J. Wang, X. Q. Ma, Q. Li, J. Britson, and L. Q. Chen, Acta Materialia **61**, 7591 (2013).
[20] C. H. Woo and Y. Zheng, Appl. Phys. A **91**, 59 (2008).
[21] S. V. Kalinin, A. N. Morozovska, L. Q. Chen, and B. J. Rodriguez, Rep. Prog. Phys. **73**, 056502 (2010).
[22] A. K. Tagantsev, L. E. Cross, and J. Fousek, *Domains in Ferroic Crystals and Thin Films* (Springer, 2010).
[23] J. Shen and Y. Q. Ma, J. Appl. Phys. **89**, 5031 (2001).
[24] N. A. Pertsev, A. G. Zembilgotov, and A. K. Tagantsev, Phys. Rev. Lett. **80**, 1988 (1998).
[25] N. A. Pertsev and H. Kohlstedt, Phys. Rev. Lett. **98**, 257603 (2007).
[26] W. J. Chen, Yue Zheng, and Biao Wang, Appl. Phys. Lett. **98**, 222902 (2011).
[27] F. A. Urtiev, V. G. Kukhar, and N. A. Pertsev, Appl. Phys. Lett. **90**, 252910 (2007).
[28] G. Gerra, A. K. Tagantsev, and N. Setter, Phys. Rev. Lett. **98**, 207601 (2007).
[29] A. K. Tagantsev, G. Gerra, and N. Setter, Phys. Rev. B **77**, 174111 (2008).
[30] R. K. Vasudevan, A. N. Morozovska, E. A. Eliseev, J. Britson, J.-C. Yang, Y.-H. Chu, P. Maksymovych, L. Q. Chen, V. Nagarajan, and S. V. Kalinin, Nano Lett. **12**, 5524 (2012).
[31] W. J. Chen, Y. Zheng, W. M. Xiong, X. Feng, Biao Wang, and Y. Wang, Sci. Rep. **4**, 5339 (2014).
[32] A. K. Tagantsev, Ferroelectrics **375**, 19 (2008).
[33] G. Akcay, S. P. Alpay, and G. A. Rossetti, J. Appl. Phys. **103**, 024104 (2008).
[34] R. Kretschmer and K. Binder, Phys. Rev. B **20**, 1065 (1979).
[35] R. R. Mehta, B. D. Silverman, and J. T. Jacobs, J. Appl. Phys. **44**, 3379 (1973).
[36] Yue Zheng, M. Q. Cai, and C. H. Woo, Acta Mater. **58**, 3050 (2010).
[37] Y. Zheng and C. H. Woo, Nanotechnology **20**, 075401 (2009).
[38] L. Q. Chen, "Landau free-energy coefficients," Phys. Ferroelectr. **105**, 363 (2007).
[39] Y. L. Li, S. Y. Hu, Z. K. Liu, and L. Q. Chen, Acta Mater. **50**, 395 (2002).
[40] D. C. Ma, Yue Zheng, and C. H. Woo, Appl. Phys. Lett. **95**, 262901 (2009).
[41] A. N. Morozovska, E. A. Eliseev, S. L. Bravina, A. Y. Borisevich, and S. V. Kalinin, J. Appl. Phys. **112**, 064111 (2012).
[42] Y. Liu, X. P. Peng, X. J. Lou, and H. Zhou, Appl. Phys. Lett. **100**, 192902 (2002).